Thermochimica Acta, 165 (1990) 261–272
Elsevier Science Publishers B.V., Amsterdam

PHASE FORMATION AND THERMAL STABILITY OF $YBa_2Cu_3O_{7-x}$ FROM COPRECIPITATED POWDERS

GERNOT BRAUN, GERHARD SCHUSTER, HELMUT ULLMANN, WOLFGANG MATZ and KARIN HENKEL

Central Institute of Nuclear Research Rossendorf, P.O. Box 19, Dresden 8051 (G.D.R.)

(Received 15 January 1990)

ABSTRACT

The calcination of coprecipitated Y–Ba–Cu oxalates and hydroxide–carbonates and of their single components were compared. The perovskite formation of $YBa_2Cu_3O_{7-x}$, and the phase transformations and decomposition of the 1–2–3 phase were investigated thermoanalytically and by X-ray diffraction. The possibilities of chemico-thermal influences on the phase formation are discussed.

INTRODUCTION

Oxide superconductors are mostly produced by mechanico-thermal means. However, powders produced by chemical coprecipitation promise some advantages, namely, low reaction and sintering temperatures, homogeneous component distribution, the production of ceramics with a high density and ordered microstructure and good processing conditions of the extensive monodisperse powders, for instance in thick layer techniques. These advantages should have a positive effect on the physical properties of the ceramic superconductor.

The first perovskitic superconductors based on La–Ba–Cu oxides were prepared by the wet chemical method of coprecipitation of the oxalates [1]. This procedure was also applied to $YBa_2Cu_3O_{7-x}$ [2,3]. The relatively high solubility of barium oxalate prevents the preparation of a precise stoichiometric product. A method of coprecipitation of yttrium and copper hydroxide with barium carbonate has therefore been developed [4]. Besides this precipitation process, calcination of the coprecipitates and formation of the 1–2–3 phase with an internal structural compound has to be optimised. The correlation between the chemico-thermal treatment and the oxygen content of $YBa_2Cu_3O_{7-x}$ is of fundamental importance for an optimum high-T_c superconductor.

The subject of this paper is the investigation of the precipitates during calcination, the formation of the 1–2–3 phase and their decomposition in

the chemico-thermal process. Our own thermoanalytical and X-ray diffraction measurements and earlier studies on the behaviour of oxalates of yttrium [5], barium [6] and copper [7], as well as of $Y(OH)_3$ [8], were compared.

EXPERIMENTAL

$YBa_2Cu_3O_{7-x}$ powder was produced using two precipitation methods.

(1) Coprecipitation of the oxalates from nitrate solutions at constant pH values. Up to 30% of the barium remained in solution. A stoichiometric 1–2–3 phase could not be obtained in this case.

(2) Coprecipitation of copper and yttrium as hydroxide, and of barium as carbonate, from a common nitrate solution by NaOH and Na_2CO_3. A very fine, weakly agglomerated powder of composition $Y_{0.98}Ba_{1.91}Cu_3O_{7-x}$ with nearly spherical particles was obtained after freeze drying. The small Ba loss can be compensated for by an excess in the initial solution.

The powder characteristics after calcination at 750 °C were: bulk density, 0.63 g cm^{-3}; toluene density, 4.87 g cm^{-3}; specific surface area (by BET), 3.3 m^2 g^{-1}; particle size d_{50}, 0.6 μm; particle distribution, 0–1.7 μm; maximum agglomerate size, 50 μm; contaminants, Na $\leqslant$ 0.1% and C = 0.58%.

The powder can be pressed at 100 MPa without milling or additions. Monophasic orthorhombic ceramics were obtained by sintering in oxygen at 935 °C and by subsequent cooling at 2.5 K min^{-1} and annealing in oxygen at lower temperatures. The crystals in the pellets were about 40 μm long and 5–10 μm wide; a dominant orientation of the crystals is obvious [4]. The density depends on the sintering time; after 24 h sintering a density of 5.4 g cm^{-3} was attained.

For comparison, the single components Y, Ba, and Cu oxalate, Y and Cu hydroxide, and $BaCO_3$ were produced and thermally treated under the same conditions as the coprecipitated products.

For the thermoanalytical investigations of the sample material, a simultaneous TG–DTG–DTA technique was applied, in which mass and thermal effects were detected dynamically and/or isothermally. Essential test values were the reaction intervals, the extrapolated onset temperatures T_e and the mass changes Δm.

The measuring conditions for calcination and formation of the 1–2–3 phase were: Mettler thermoanalyser TA-1 with Pt–PtRh DTA crucible holder and quartz or PtRh10 cup crucible; heating/cooling rate, 6 K min^{-1}; maximum temperature, 1400 °C; gas atmosphere, 5 l h^{-1} oxygen (dry); sample mass, 100 mg; reference, Al_2O_3.

The measuring conditions for the phase transformation were: Netzsch thermoanalyser STA 429 with heat-flux DTA crucible holder and Pt crucible; heating/cooling rate: 10 and 20 K min^{-1}; maximum temperature,

970 °C; gas atmosphere, air (dry), static; sample mass, 54 mg; reference, Al_2O_3.

The buoyancy effects were considered by comparative measurements under inert conditions.

For the X-ray diffractometry the precipitate and superconductor materials were annealed at various temperatures in oxygen and quenched in air. The structures formed were measured at room temperature using the URD-6 and HZG-4 counter-tube goniometers, respectively, and Cu $K\alpha$ radiation. In order to ensure that the quenched-in structure was representative for the annealing temperature, in situ X-ray diffraction was performed by the Guinier technique in the temperature range up to 925 °C.

RESULTS

Calcination of the precipitates and formation of the precursor

The oxalate precipitates lose adsorbed or crystal water in a graduated process, see Fig. 1 and Table 1. The dehydration continues to the start of the oxalate decomposition. It is therefore difficult to assign the mass changes precisely to the individual reactions.

CuC_2O_4 decomposition occurs in a single step to CuO without intermediate carbonate formation. Because of the reducing effect of CO on Cu^{2+}, some Cu_2O is formed ($T_e = 245$ °C); this is not stable in this temperature range and rapidly reoxidises ($T_e = 355$ °C). CuO melts only above 1000 °C ($T_s = 1030$ °C) or is reduced endothermally to Cu_2O, which is stable at this temperature. $Y_2(C_2O_4)$ decomposes in several steps. The oxalate decomposition ($T_e = 350$ °C) is exothermically justified by simultaneous CO oxidation and overlaps with the endothermic carbonate decomposition. Consequently the latter reaction appears to be exothermal. The thermal decomposition of BaC_2O_4 proceeds in a few steps. During decomposition to carbonate ($T_e = 450$ °C), CO is formed [9] and is immediately oxidised to CO_2 in an oxygen atmosphere. At 800 °C the rhombic modification of $BaCO_3$ changes in two stages to the hexagonal form which then decomposes endothermally to BaO ($T_e = 1040$ °C).

During the calcination of the coprecipitated oxalate pre-dried at 20 °C, BaC_2O_4 first dehydrates in two stages ($T_e = 65$ °C). Above 200 °C the coprecipitated oxalate decomposes exothermally in several steps with CO_2 emission; first, CuC_2O_4 rapidly to CuO, and BaC_2O_4 to $BaCO_3$ ($T_e = 230$ °C), followed by $Y_2(C_2O_4)_3$ in two overlapping stages to $Y_2(CO_3)_3$ and Y_2O_3 ($T_e = 355$ and 495 °C respectively). The calcination process of the formation of the precursor consisting of Y_2O_3, CuO and $BaCO_3$ is complete at 500–600 °C.

The main decomposition stages of the single oxalates appear in the

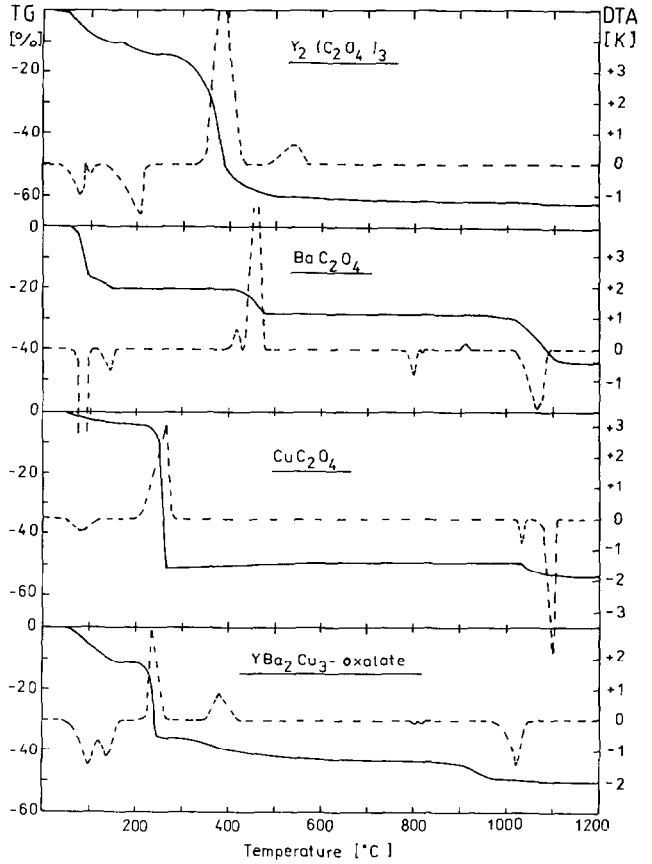

Fig. 1. TG/DTA calcination of oxalates (single components and 1–2–3 oxalate coprecipitate). $q = 6$ K min^{-1}.

coprecipitated product at approximately the same temperatures; the magnitude of the effects corresponds to the mass ratios of the 1–2–3 product. The phase transformation of $BaCO_3$ can be distinctly observed at 800 °C. It is completely decomposed during the first heating up to 950 °C. The clear DTA effect no longer appears during repeated heating.

The hydroxide–carbonate precipitated products are first dried and dehydrated in steps (Fig. 2, Table 1). The gel-shaped $Cu(OH)_2$ is dehydrated in one step in a wide temperature range ($T_e = 145$ °C). Above 1000 °C, CuO is slowly reduced, without melting, to Cu_2O ($T_e = 1095$ °C). The gel-shaped $Y(OH)_3$ is endothermally dehydrated step-wise over a wide temperature range ($T_e = 390$ °C, 480 °C, and completely above 600 °C to the oxide). Finally, after the rhombic-to-hexagonal phase transformation, the microcrystalline $BaCO_3$ has already endothermally decomposed with emission of CO_2 above 1000 °C ($T_e = 1030$ °C), accelerated by the flowing gas, although the decomposition pressure of pure $BaCO_3$ reaches 1×10^5 Pa only at 1400 °C [10].

TABLE 1

Thermoanalytical calcination of the precipitates in oxygen [a]

Precipitate	Reaction				
	Evaporation of adsorbed and crystal water		Decomposition of oxalate or hydroxide		Decomposition of carbonate
CuC_2O_4	30–140 °C $\Delta m = -3.4\%$		140–265 °C $\Delta m = -47.5\%$ in one step to CuO/Cu_2O		
$Y_2(C_2O_4)_3$	35–240 °C $\Delta m = -14.1\%$		240–500 °C $\Delta m = -41.6\%$		500–740 °C $\Delta m = -5.6\%$
BaC_2O_4	60–150 °C $\Delta m = -19.9\%$		395–480 °C $\Delta m = -8.9\%$		930–1125 °C $\Delta m = -15.1\%$
YBa_2Cu_3 oxalate	30–170 °C $\Delta m = -11.7\%$			205–1040 °C $\Delta m = -37.8\%$	
$Cu(OH)_2$		40–165 °C (745 °C) $\Delta m = -15.6\%$			
$Y(OH)_3$	20–335 °C $\Delta m = -17.6\%$		335–590 °C $\Delta m = -15.1\%$		
$BaCO_3$					995–1000 °C $\Delta m = -18.0\%$
YBa_2Cu_3 hydroxide–carbonate		20–620 °C $\Delta m = -12.0\%$			620–1085 °C $\Delta m = -11.2\%$

[a] All Δm values refer to initial mass.

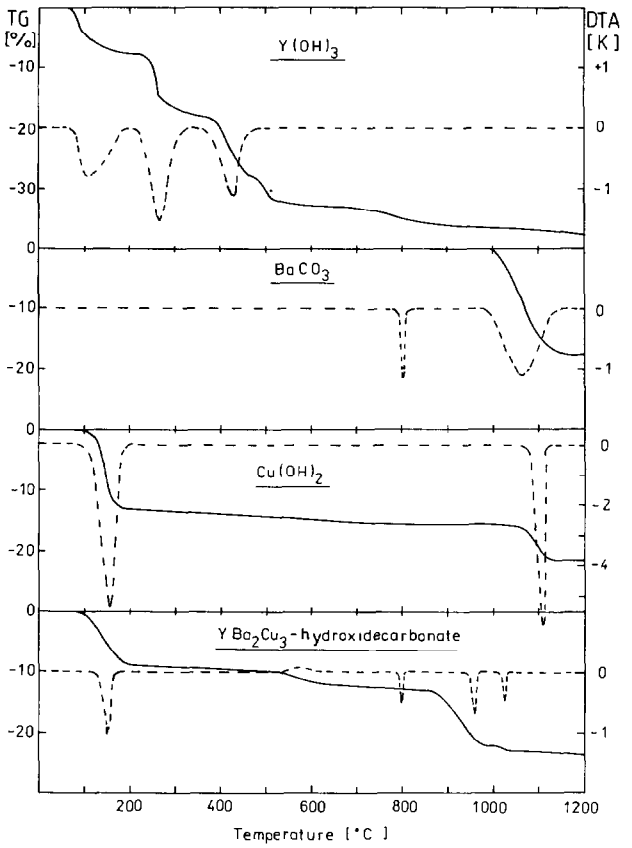

Fig. 2. TG/DTA calcination of hydroxides and carbonates, respectively (single components and 1–2–3 hydroxide–carbonate coprecipitate). $q = 6$ K min^{-1}.

In contrast to the coprecipitated oxalate, the main decomposition stages of single components do not appear in the coprecipitated hydroxide–carbonate. The product pre-dried at 60 °C is first completely dried, and the $Cu(OH)_2$ is dehydrated during calcination ($T_e = 105$ °C). Decomposition of $Y(OH)_3$ to YO(OH) has probably already begun at this stage, finally yielding Y_2O_3 above 365 °C. An exothermic DTA effect overlays this reaction ($T_p = 575$ °C, possibly the formation of an intermediate phase, see below). Exothermic effects between 200 and 400 °C caused by oxidation of Cu^+ to Cu^{2+} (analogous to the calcination of CuC_2O_4 [11]) could not be found for the coprecipitated hydroxide–carbonate. Calcination is complete at about 600 °C and results in a precursor with some amorphous and some crystalline structure consisting of Y_2O_3, CuO and $BaCO_3$ in a loose bonding. Isolated $BaCO_3$ or $BaCO_3$ adsorbed on the Y–Cu hydroxide has not yet been found in the calcination product (phase transformation at 800 °C); it is completely decomposed during the first heating to 950 °C (no DTA effect with repeated heating).

Figure 3 shows the X-ray diffraction spectra of the coprecipitated Y–Ba–Cu hydroxide–carbonate. The sample dried at 50 °C shows some broad, unresolved reflections of $BaCO_3$ (24°) and CuO. The line-broadening is caused by the small crystallite size. At 400 °C the Bragg peaks sharpen, indicating growth of the crystallites. Such step-wise changes in the microstructure were also detected by emanation thermal analysis (ETA) of the coprecipitated oxalates in the range between 300 and 750 °C [12]. At 550 °C, Y_2O_3 reflections occur; at 650 °C additional peaks appear (marked by arrows in Fig. 3), which are produced from an intermediate phase (identified as $Y_2Cu_2O_5$ according to ref. 13; see also the exothermic DTA shoulder at 575 °C). The peaks of the initial products become sharper with further crystal growth.

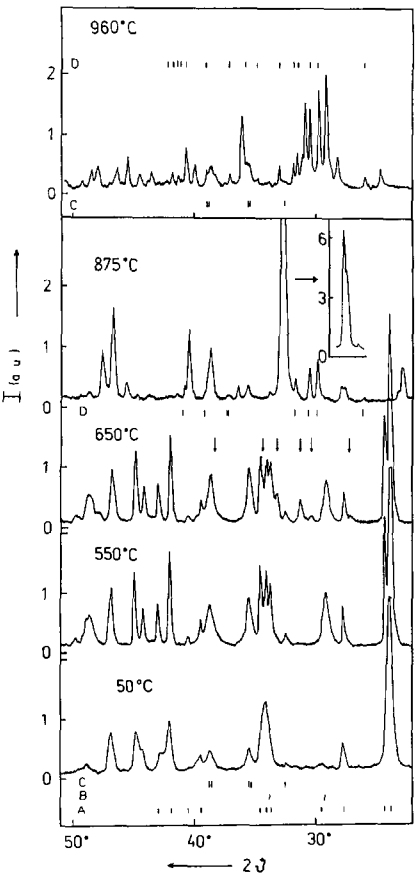

Fig. 3. X-ray diffraction patterns of coprecipitated YBa_2Cu_3 hydroxide–carbonate powder annealed at different temperatures for 1 h in O_2 and quenched to 20 °C in air. The main reflections of the phases are: A, $BaCO_3$; B, Y_2O_3; C, CuO; D, $BaCuY_2O_5$; arrows, $Cu_2Y_2O_5$.

Formation and phase changes of the perovskite structure

The formation of the perovskite phase from the precursor takes place in a complex endothermic reaction [14]. The decomposition of the $BaCO_3$ [15] begins above 600 °C, both in the mixed hydroxide–carbonate and the mixed oxalate (T_e = 895 and 875 °C respectively) and is complete by 980 °C. The decomposition of the isolated $BaCO_3$ begins above 1000 °C. The three-component reaction of the perovskite formation of the coprecipitated product consequently favours the decomposition of the carbonate and shifts this to lower temperatures. In an inert atmosphere (N_2, He, vacuum), the $BaCO_3$ decomposition is accelerated and the temperature of the formation of the 1–2–3 phase is lowered [16]. In the same temperature range, the two-component reactions, Y/Cu–O and Ba/Cu–O [17], compete with this three-component reaction. Therefore, the homogeneity and small particle size of the initial materials promote the formation of the monophasic superconductor.

According to the in situ X-ray diffraction investigations, the formation of the orthorhombic $YBa_2Cu_3O_{7-x}$ phase begins at 830 °C. At 875 °C it is already the main constituent (main reflection at 32–33°); in addition, small quantities of CuO and of the green phase, $BaCuY_2O_5$, (D reflections in Fig. 3) are found. When the annealing temperature is increased to 935 °C, formation of the 1–2–3 phase is accelerated and the portion of green phase is reduced. A monophasic orthorhombic material is obtained after an annealing time of 24 h in oxygen at 935 °C.

The formation reaction of the 1–2–3 phase overlaps with the beginning of its peritectic decomposition (melting and phase separation [18], T_e (DTA) = 950 and 1010 °C, Fig. 2). This is combined with an additional oxygen release, which is higher for the hydroxide–carbonate-precipitated than for the oxalate-precipitated $YBa_2Cu_3O_{7-x}$. After one hour of annealing at 960 °C, the 1–2–3 phase is almost completely decomposed to the Y-rich green phase, $BaCuY_2O_5$, to CuO, and to some unidentified phases (Fig. 3). This process is extensively reversible on cooling, provided the material is not heated much above 1050 °C. The decomposition products form a ternary eutectic phase in the system $YO_{1.5}$–BaO–CuO [19], in which, above 1000 °C, $BaCuO_2$ decomposes continuously and reversibly to BaO and CuO/Cu_2O. A double peak occurs on cooling this phase mixture (hysteresis, 965 and 900 °C), and this supports the interpretation of this high temperature reaction as being a phase transformation. On further heating above 1200 °C, the green phase, $BaCuY_2O_5$, decomposes irreversibly to Y_2O_3, $BaCu_2O_2$ and CuO/Cu_2O (T_e (TG) = 1205–1255 °C and T_e (DTA) = 1235–1270 °C, depending on the powder quality), in agreement with ref. 19, but contrary to ref. 20. On cooling, an exothermic DTA peak can no longer be observed and no superconducting phase is formed.

Monophasic $YBa_2Cu_3O_{7-x}$, on heating in air at about 430 °C and cooling at 628 °C, undergoes a reversible phase transformation (Fig. 4).

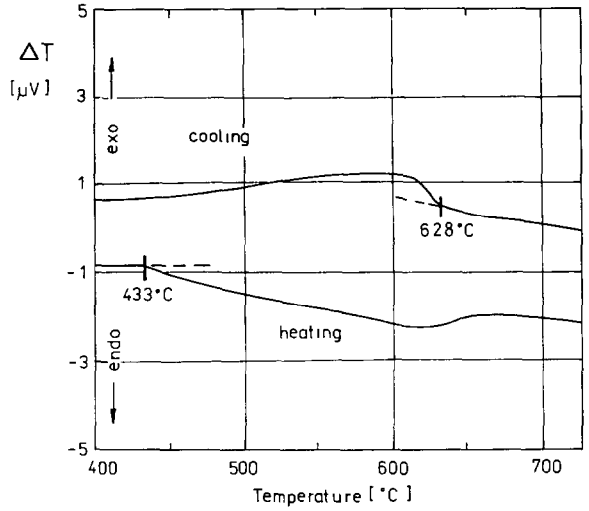

Fig. 4. Heat flux DTA of $YBa_2Cu_3O_{7-x}$ (annealed for 24 h in O_2 at 935°C, slowly cooled) on heating and cooling in air.

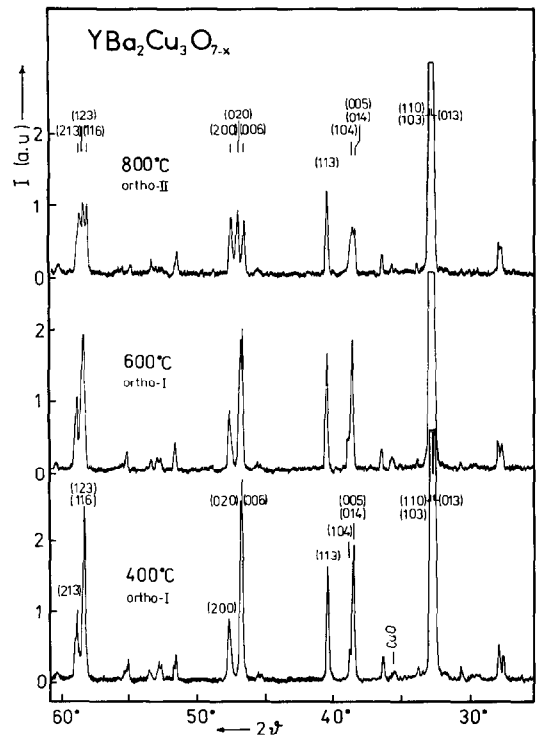

Fig. 5. X-ray diffraction patterns of $YBa_2Cu_3O_{7-x}$ annealed at different temperatures for 16 h in O_2.

Simultaneously, oxygen is reversibly exchanged in the same temperature region and above it. The maximum oxygen content of the sample (the smallest x value) is present at the beginning of the phase transformation during heating. X-ray diffraction of the $YBa_2Cu_3O_{7-x}$ annealed at 400 °C and also at 600 °C shows the expected orthorhombic structure (*o*-I) (Fig. 5). In contrast the 800 °C sample has changed to another *o*-structure (*o*-II), for which the difference in the lattice constants, $a - b$, is smaller than that of the normal *o*-structure, but does not correspond to the tetragonal structure. These aspects are variously covered in the literature [21–25].

DISCUSSION AND CONCLUSIONS

Table 2 summarises the thermoanalytical and X-ray diffraction results of the calcination of the coprecipitated Y–Ba–Cu hydroxide–carbonate and of the 1–2–3 phase formation. The drying and the decomposition determine the calcination process, which is completed between 500 °C and 600 °C. The different precipitating and drying processes influence the calcination only slightly. The resulting precursor of Y_2O_3, CuO and $BaCO_3$ has some X-ray-amorphous and some microcrystalline structure. In the case of the hydroxide–carbonate, there is a loosely bound coprecipitated product. The precipitates of the oxalates, however, form a mixture of the single components. The reversible oxygen exchange of the freshly calcined, coprecipitated hydroxide–carbonate [26] is a characteristic which indicates that formation of the superconducting phase has taken place.

The crystal growth of the oxides and the carbonate, and the possible phase separation and formation of the intermediate phases from the previously homogeneous precursor towards the end of the calcination, is undesirable for optimum perovskite phase formation. Therefore a higher heating rate through this critical temperature range (550–700 °C) is desirable.

Decomposition of the homogeneous ultrafine precursor, and formation of the 1–2–3 phase begin in oxygen at 830 °C in a uniform, non-diffusion-controlled phase-boundary reaction [27]. It proceeds from the surface to the inside of the particles, and its rate depends on the reaction surface area. An increase in the annealing or sintering temperature to 935 °C accelerates the formation of the 1–2–3 phase and leads to the monophasic product.

If coprecipitated fine hydroxide–carbonate powder is used as a starting material, then with a longer sintering time (24 h) the sintering temperature can be lowered to the real temperature of the perovskite formation. In this way the complex decomposition of the 1–2–3 phase is avoided.

The reversible structure change of the 1–2–3 phase between 430 and 630 °C (in air) with continuous oxygen exchange was detected by X-ray diffraction as an order–disorder transformation of two orthorhombic phases due to a change in the oxygen stoichiometry. The ordered phase corresponds

TABLE 2

Thermoanalytical and X-ray diffraction results of the calcination of coprecipitated Y–Ba–Cu hydroxide–carbonate and of the 1–2–3 phase formation

TG							
React. range $T_i - T_f$	(°C)	20–365	365–620		620–995	995–1085	1165–1315
Onset temp. T_e	(°C)	105	370		895	1005	1255
Mass change Δm	(%)	−9.6	−2.4		−10.1	−1.1	−0.4
DTA							
Heat of reaction		endothermic	exothermic	endothermic	endothermic	endothermic	endothermic
Peak temp. T_p	(°C)	150	565	795	960	1025	1275
Peak height $(DTA)_p$	(K)	−1.0	+0.1	−0.5	−0.7	−0.5	−0.2
X-ray diffraction							
Temperature range	(°C)	20–400	400–550	600–700	875–935	> 960	> 1200
Identified phases		$BaCO_3$, CuO	$BaCO_3$, CuO	CuO, Y_2O_3, $BaCO_3$, $Y_2Cu_2O_5$	$YBa_2Cu_3O_7$, $BaCuY_2O_5$, CuO	$BaCuY_2O_5$, $BaCuO_2$, CuO	CuO, Y_2O_3, $BaCu_2O_2$
Interpretation		Drying Dehydration ←——Decomposition——→		$BaCO_3$ transformation + intermediate phase	Perovskite phase formation + peritectic melting and decomposition	Peritectic melting + decomposition of 1–2–3 phase and their resultant products with O_2 release	

to the 90-K superconductor. This transformation is caused by the volume increase in the unit cell of $YBa_2Cu_3O_{7-x}$ due to the thermal loss of oxygen [28] (o-I = 173.7 Å^3, o-II: 174.1 Å^3, according to our X-ray measurements). Therefore the oxygen stoichiometry decides the obtained structure.

REFERENCES

1 J.G. Bednorz and K.A. Mueller, Z. Phys. B, 64 (1986) 189.
2 T. Kawai and M. Kanai, Jpn. J. Appl. Phys., 26 (1987) L736.
3 K. Kaneko, H. Ihara, M. Hirabayashi, N. Terada and K. Senzaki, Jpn. J. Appl. Phys., 26 (1987) L734.
4 B. Rauschenbach, C. Neelmeijer, G. Schuster, P. Knothe and W. Erfurth, Crystal Res. Techn. (Berlin), in press.
5 K.G. Nair, V.V. Sreerajan, V.S.V. Nayar and C.G.R. Nair, Thermochim. Acta, 39 (1980) 253.
6 A.S. Bhatti, D. Dollimore and A. Fletcher, Thermochim. Acta, 78 (1984) 63 and 217.
7 J. Mu and D.D. Perlmutter, Thermochim. Acta, 49 (1981) 207.
8 T. Sato, I. Satoshi and K. Sato, Thermochim. Acta, 133 (1988) 79.
9 H. Tanaka and N. Koga, J. Therm. Anal., 32 (1987) 1521.
10 H. Remy, Lehrbuch Anorg. Chem., Akad. Verlagsges. Geest and Portig, Leipzig, 1957, S. 330.
11 J. Šesták, T. Hanslik, M. Nevřiva, D. Zemanova, E. Pollert, A. Tříska and J. Tlaskal, J. Therm. Anal., 33 (1988) 947.
12 V. Balek and J. Šesták, Thermochim. Acta, 133 (1988) 23.
13 PDF-Chart N° 33-511, JCPDS, Swarthmore, PA 19081, USA.
14 P. Kishan, L.K. Nagpaul and S.N. Chatterjee, Solid State Comm., 65 (1988) 1019.
15 A. Negishi, Y. Takahashi, R. Sakamoto, M. Kamimoto and T. Ozawa, Thermochim. Acta, 132 (1988) 15.
16 J.J. Rha, K.J. Yoon, S.L. Kang and D.N. Yoon, J. Am. Ceram. Soc., 71 (1988) C-328.
17 M. Kamimoto, R. Sakamoto, A. Negishi, Y. Takahashi and M. Hirabayashi, Thermochim. Acta, 142 (1989) 281.
18 T. Ozawa, A. Negishi, Y. Takahashi, R. Sakamoto and H. Ihora, Thermochim. Acta, 124 (1988) 147.
19 M. Nevřiva, E. Pollert, J. Šesták, L. Matejkova and A. Tříska, Thermochim. Acta, 127 (1988) 395.
20 D.M. de Leeuw, C.A.H.A. Mutsaers, G.P.J. Geelen, H.C.A. Smoorenburg and C. Langereis, Physica C, 152 (1988) 508.
21 P.K. Gallagher, H.M. O'Bryan, S.A. Sunshine and D.W. Murphy, Mat. Res. Bull., 22 (1987) 995.
22 A.G. Khachaturyan and J.W. Morris, Jr., Phys. Rev. Lett., 61 (1988) 215.
23 J.D. Jorgensen, M.A. Beno, D.G. Hinks, L. Soderholm, K.J. Volin, R.L. Hitterman, J.D. Grace and I.V. Schuller, Phys. Rev. B. 36 (1987) 3608 and 5731.
24 G. Balestrino, S. Barbanera, P. Paroli and G. Paterno, Physica Scripta, 37 (1988) 907.
25 S.R. Dharwadkar, V.S. Jakkal, J.V. Yakhmi, I.K. Gopalakrishnan and R.M. Iyer, Solid State Comm., 64 (1987) 1429.
26 G. Braun, K. Henkel, G. Schuster, K. Teske, W. Matz and H. Ullmann, Wiss. Beitr. FSU Jena, Therm. Anal. Methods Ind. Res., 4, submitted.
27 M. Kamimoto and T. Ozawa, Thermochim. Acta, submitted.
28 W. Wong-Ng, R.S. Roth, L.J. Swartzendruber, L.H. Bennett, C.K. Chiang, F. Beech and C.R. Hubbard, Advan. Ceram. Mater., 2 (1987) 565.